Genetically-Encoded Discovery of Proteolytically Stable Bicyclic Inhibitors of Morphogen NODAL

Jeffrey Y. K. Wong,[1] Raja Mukherjee,[1] Olena Bilyk,[2] Jiayuan Miao,[3] Vivian Triana,[1] Mark Miskolzie,[1] Yu-Shan Lin,[3] Antoine Henninot,[4] John J. Dwyer,[4] Serhii Kharchenko,[5] Anna Iampolska,[5] Dmitriy Volochnyuk,[5] Lynne Postovit[2] and Ratmir Derda[1*]

1. Department of Chemistry, University of Alberta, Edmonton, AB T6G 2G2, Canada

2. Department of Oncology, University of Alberta, Edmonton, AB T6G 2G2, Canada

3. Department of Chemistry, Tufts University, Medford, MA 02155, USA

4. Ferring Research Institute, San Diego, California 92121, USA

5. Enamine Ltd., Chervonotkatska Street 78, Kyiv 02094, Ukraine

*Corresponding author: ratmir@ualberta.ca

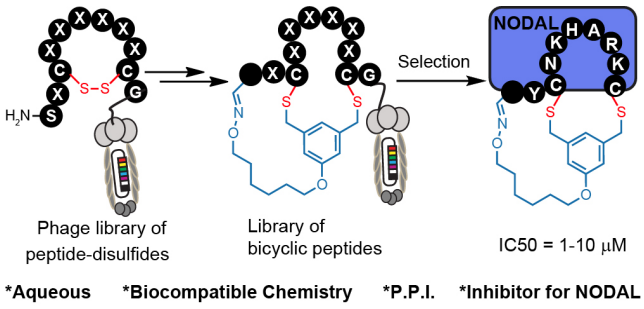

ABSTRACT: In this manuscript, we developed a Two-fold Symmetric Linchpin (**TSL**) that converts readily available phage display peptides libraries made of 20 common amino acids to genetically-encoded libraries of bicyclic peptides displayed on phage. **TSL** combines an aldehyde-reactive group and two thiol-reactive groups; it bridges two side chains of cysteine [C] with an N-terminal aldehyde group derived from the N-terminal serine [S], yielding a novel bicyclic topology that lacks a free N-terminus. Phage display libraries of $SX_1CX_2X_3X_4X_5X_6X_7C$ sequences, where X_i is any amino acids but Cys, were converted to a library of bicyclic **TSL**-[S]X_1[C]$X_2X_3X_4X_5X_6X_7$[C] peptides in 45 ± 15% yield. Using this library and protein morphogen NODAL as a target, we discovered bicyclic macrocycles that specifically antagonize NODAL-induced signaling in cancer cells. At a 10 μM concentration, two discovered bicyclic peptides completely suppressed NODAL-induced phosphorylation of SMAD2 in P19 embryonic carcinoma. The **TSL**-[S]Y[C]KRAHKN[C] bicycle inhibited NODAL-induced proliferation of NODAL-Tky-nu ovarian carcinoma cells with apparent IC50 1 μM. The same bicycle at 10 μM concentration did not affect the growth of the control Tky-nu cells. **TSL**-bicycles remained stable over the course of the 72 hour-long assays in a serum-rich cell-culture medium. We further observed general stability in mouse serum and in a mixture of proteases (Pronase^{TM}) for 33 diverse bicyclic macrocycles of different ring sizes, amino acid sequences, and cross-linker geometries. **TSL**-constrained peptides expand the previously reported repertoire of phage display bicyclic architectures formed by cross-linking Cys side chains. We anticipate that it will aid the discovery of proteolytically-stable bicyclic inhibitors for a variety of protein targets.

INTRODUCTION

23 out of the 60 FDA approved peptide drugs are peptide macrocycles.[1] Macrocyclization of peptides increases binding affinity,[2] improves permeability through the cell membrane[3-4] and stability towards enzymatic hydrolysis[5-6] compared to linear peptides.[7-8] The large surface area of macrocycles has been critical for identifying molecules that bind extended protein surfaces and inhibit protein-protein interactions.[4] Introduction of a bridgehead into macrocyclic topologies to form so-called bicyclic peptides could further decrease conformational flexibility and increase stability or binding potency. [9-10] Bioactive bicyclic peptides that have been reported thus far originate from natural products,[11] computational approaches,[12] cyclization of known bioactive peptides,[13-15] or screening of combinatorial libraries.[16-17] To fuel the last method, synthesis on the solid support can yield libraries of 10^2–10^6 diversity,[16-17] and DNA-encoded libraries[18-20] or late-stage chemical diversification of biosynthesized peptides displayed on mRNA[21] or phage[22-26] can give rise to libraries with 10^9–10^{12} diversity.[27] Development of new approaches for chemical diversification of mRNA and phage display libraries[27-28] make it possible to screen and discover new macrocyclic and bicyclic topologies with value-added properties. In this manuscript, we develop a methodology for late-stage chemical diversification of phage display peptide libraries to create previously unexplored genetically-encoded libraries of new, "terminus-to-side chain" bicyclic topology.

There are currently two strategies for synthesizing phage display bicyclic libraries: Both of them employ cross-linking of Cys side chains with electrophiles (Figures 1A). They can be divided into two sub-categories: (i) Cross-linking of three Cys residues with a C_3-symmetric electrophile to yield bicycles displayed on phage[5] (Figure 1A); (ii) Cross-linking of four Cys residues with C_2-symmetric electrophiles to yield a mixture of three regioisomeric bicycles displayed on phage[29] (Figure 1A). Bicyclic libraries have also been synthesized in mRNA display libraries using strategy (i) or via incorporation of two pairs of orthogonally reactive unnatural amino acids (UAAs) into mRNA display libraries.[30-31] Incorporation of UAAs

into phage display libraries has been reported and UAAs have been used to generate a phage display macrocyclic libraries.[32-35] In this manuscript, we sought to devise the modification approach that uses peptide libraries made of 20 common amino acids: Bypassing the complexity of UAA incorporation avoids biases that might result from the incorporation of such UAAs in the phage library.[36] We combined well-established modification of phage display libraries with N-terminal Ser and Cys-side chains to generate a novel genetically-encoded bicycles topology. This topology does not display a free N-terminus and unlike previous reported strategy(ii), this strategy yield a single regioisomer. (Figure 1B).

Aldehyde is a versatile bio-orthogonal handle. In proteins, aldehyde can be incorporated by periodate oxidation of N-terminal Ser.[37-38] This method has been used for modifications of peptides,[39] for PEGylation of clinically relevant growth factors and cytokines to improve their stability in preclinical studies,[40] and for synthesis of antibody-drug conjugates.[41-42] Libraries with N-terminal Ser have been previously converted to peptide-aldehydes and modified by oxime and hydrazine,[43-44] benzamidoxime,[45] or Wittig reaction[46] and used for selection of diverse chemically-modified peptide ligands.[43-51] Our report provides the first example of using this versatile technology for bicyclization. To this end, we devised a macrocyclization approach that employed an N-terminal aldehyde residue. To demonstrate the value of such a library in discovering new bioactive bicycles, we employed this library to discover inhibitors of protein NODAL and antagonists of NODAL-induced signaling.

The extracellular embryonic morphogen NODAL belongs to the transforming growth factor-beta (TGF-β) superfamily. It is a stem-cell-associated factor that has emerged as a putative target for the treatment of cancer.[52-62] NODAL is normally restricted to embryogenesis, wherein it maintains pluripotency in the epiblast and governs the formation of the body axis and left-right asymmetry.[63-65] After development, NODAL is relatively restricted to reproductive cell types and is not detectable in most normal adult tissues.[63-64,66] However, NODAL expression re-emerges in a large number of divergent cancers.[52-62] In almost every cancer studied thus far, the acquisition of NODAL expression is associated with increased

tumorigenesis, invasion, and metastasis. It supports self-renewal in pancreatic and breast cancer stem cells and is enriched in breast,[67] prostate,[58] melanoma,[56] pancreatic,[68] colon,[54] and ovarian[50,60] cancer cells with stem-cell properties. NODAL exerts its function by binding to and activating the cell surface receptors Alk4 and Alk7 in cooperation with the co-receptors Cripto-1 (FDGF1) or Cryptic (CFC1) to form a ligand–receptor complex that leads to the phosphorylation of Smad2/3 and the transcription of target genes, including NODAL itself. The only available inhibitor of NODAL to date, monoclonal anti-NODAL antibody 3D1,[69] has demonstrated success in preclinical models of melanoma and is currently undergoing further preclinical evaluation. No small-molecule or macrocyclic inhibitors of NODAL are presently available. In this manuscript, we employed bicyclic phage libraries to discover the first in class bicyclic ligands for NODAL protein. These ligands antagonize NODAL-induced signaling and specifically suppress NODAL-promoted proliferation of cancer cells. Evaluation of these antagonists benefited from the unique topology of the macro-bicycles that masked the N-terminus and equipped these macro-bicycles with multi-day stability in serum-rich cell culture media.

RESULTS AND DISCUSSION

Optimization of bicyclization on unprotected synthetic peptides. The chemical linkers **TSL-1**, **TSL-3**, and **TSL-6** containing aminooxy and benzyl chloride functional groups (Figure 2A) were synthesized (Scheme S1) and tested for their ability to modify a series of unprotected peptides of structure SX_nCX_mC where X is any amino acids except Cys and n+m ranges from 3 to 12. To mimic the conditions that would be suitable for modification of phage displayed library of peptides, we used model peptides at the micromolar concentration in aqueous buffers and treated them with super-stoichiometric reagents (Figure 2B). Figures 2C–2D described monitoring of the reaction progress between a representative model peptide SICRFFCGGG (200 μM) and $NaIO_4$ (2.4 mM) to form the N-terminal oxoaldehyde. Quenching the excess of $NaIO_4$ with an excess of methionine, decreasing the pH of the reaction, and addition of 1 mM **TSL-6**

formed the oxime (Figure 2B). At pH ranging from 2.0 to 3.5, the rate constant of this ligation was k = 0.81–0.93 $M^{-1}s^{-1}$.(Figures 2C–2D). In these conditions, oxime ligation was complete within 1 hour. Increasing the pH to 4.5 decreased the rate (k = 0.37 $M^{-1}s^{-1}$) and led to only partial completion in 1 hour (Figure 2D). Little to no oxime was formed at a higher pH (Figure 2D). We note that aniline can catalyze oxime reactions[51,70]; however, we avoided aniline and other nucleophilic catalysts to prevent the formation of byproducts with **TSL-6**.[71] The addition of 1 mM TCEP to the ligated product reduced the disulfide linkage. Raising the pH to 10 led to bicyclization of peptides in 3 hours.

This reaction successfully modified 28 unique peptides of different spacing between the Ser and Cys residues with an average isolated yield of 40% (Figure 2E). The yields for 33 bicycles are summarized in Table S1, products modified with **TSL-6**, **TSL-1** and **TSL-3** are denoted as **#b**, **#c** and **#d** respectively. Additional characterization of **TSL**s modified peptides can be found in Schemes S2–S35. The 28 unique model peptides were selected either at random (**1a**–**3a**, **6a**–**9a**, and **25a–28a**) or chosen in the phage display selection (**4a–5a** and **14a–21a**). Two peptides (**12a–13a**) were adapted from a previous publication.[72] Table S2 further highlights the various physicochemical properties of these peptides. We compared the yields of this reaction to modification of peptides with other reagents such as pentafluorophenyl sulfide **(PFS),** 1,3,5-tris(bromomethyl)benzene (**TBMB**), and α,α′-dibromo-m-xylene (**DBMB**). **PFS** cyclized peptides had an average yield of 35.5% (Scheme S36). **TBMB** cyclized peptides had an average yield of 35% (Schemes S37–S38). **DBMB** cyclized peptides had an average yield of 31% (Table S3). In conclusion, the aqueous biocompatible modification of peptides with **TSL** effectively produced bicyclic peptides with yields compatible with other reagents used in peptide cyclization or bicyclization. Although oxime linker is known to be reversible, we observed these bicycles to be stable in aqueous ammonium acetate (pH 4.7), PBS (pH 7.4), and Tris (pH 8.5) buffers for a month at room temperature (Figure S1).

Modification of phage display libraries. The bicyclization approach described above was compatible with the modification of the phage display peptide libraries. To quantify the efficiency of bicyclization

reaction in phage libraries, we used biotinylation and phage capture steps similar to approaches employed in previous publications (Figure 3).[43-46] Previously, formation and reactivity of aldehyde in phage libraries was quantified by exposing the library to an aldehyde-reactive aminooxybiotin (AOB) and counting the number of biotinylated particles captured by streptavidin paramagnetic particles ("AOB capture," Figure S2C).[51] Using the reported oxidation conditions, we exposed a phage displaying $SX_1C\ X_2X_3X_4X_5X_6X_7C$ library of 10^8 peptides to an ice-cold solution of $NaIO_4$ (60 μM in PBS) for 9 min, quenched the oxidation by 0.5 mM methionine for 20 min and used AOB capture to confirm that 93±11% of the library was converted to aldehyde. Reacting with 1 mM solution of linchpin **TSL-6** at pH 3.5 for 1 hour consumed most of the aldehyde functionalities (Figure S2E). After removing excess **TSL-6** by size exclusion spin column, we exposed the phage to a biotin-thiol reagent (BSH, Figure 3E) and captured the biotinylated clones by streptavidin paramagnetic particles. This "BSH capture" confirmed that 52±4% of the library contained thiol-reactive benzyl chloride groups (Figure 3B). Exposure of phage to TCEP and then pH 10 buffer completed bicyclization as evidenced by the decrease in BSH capture. In the control condition, incubation of the **TSL-6** ligated library at pH 10 in the absence of TCEP did not lead to any decrease in BSH capture, indicating that the number of benzyl chloride groups on phage remained unchanged in the absence of TCEP. We estimated 41±13% of library to be converted to **TSL6**-bicyclic library (Figure 3D). Detailed calculation of the conversion percentage can be found in Figure S3. Similar monitoring of the modification of the $SX_1C\ X_2X_3X_4X_5X_6X_7C$ library with **TSL-1** and **TSL-3** (Figure S4) and the $SX_1C\ X_2X_3X_4C$ phage with **TSL-6** (Figure S5) demonstrated a generality of this approach.

The ligation condition showed minor effects on the infectivity of the phage (Figure S3). To confirm that the chemical modification did not compromise the integrity of the phage DNA, we performed PCR (Figure S6) of the library and deep sequenced the PCR amplicons to monitor the sequence diversity of the library before and after chemical modification. If chemical modification significantly damaged the DNA, we anticipated observing a change in library composition. As the composition of the library before and

after the modification remained the same (Figures S7–S9), we concluded that the modification did not impact the diversity of the phage library and did not impact the integrity of the phage DNA. These studies collectively demonstrate the construction of a library of 10^8 bicycles that offer the potential for discovering bicyclic ligands for any target using canonical selection approaches.

Selection of bicycles that bind to NODAL. We applied a **TSL-6**-modified phage display library $SX_1C X_2X_3X_4X_5X_6X_7C$ to discover a ligand for the morphogen NODAL. We performed three rounds of phage selection using His_6-tagged NODAL protein as the bait. In between rounds of selection, we raised the stringency by increasing the number of washes and reducing the amount of immobilized NODAL protein (Figure 4A). In round 3, we also performed two control selections; in first control, we panned the unmodified R3 library against the NODAL protein (R3-UN) and in second control, we panned the **TSL-6**-modified R3 library against unrelated His_6-tagged protein (R3-TG). Phage recovery increased in R3 when compared to R1 and R2. This recovery was ablated by 20-fold when the unmodified round 3 library was panned against NODAL (R3-UN) and when the **TSL-6**-modified library was panned against unrelated protein (R3-TG) (Figure 4B). Deep sequencing the output of all selection round and the control experiments identified families of sequences that exhibited high normalized abundance in R3 and low normalized abundance in R1, R2, and control experiments R3-UN, and R3-TG (Figures 4B and S10). From these families, we selected six representative sequences for further validation (**14a**–**19a**; Figures 4B and S10).

Validation of NODAL bicyclic inhibitors. The bicycles **14b**–**19b** were chemically synthesized and tested for their ability to antagonize NODAL-induced signaling in a previously established P19 cell line.[75-76] Stimulations of the P19 cells with rhNODAL at 100 ng/mL for 1 hour led to the phosphorylation of SMAD2 (Figure 4D, column 3). This phosphorylation was inhibited by ALK4/7 kinase inhibitor SB431542 (Figure 4D, column 4), as previously reported.[58,73-74] Bicyclic peptides **14b**–**19b** at 100 μM were able to inhibit rhNODAL-induced phosphorylation of SMAD2 (Figure S11A). At the concentration of 10 μM, bicyclic peptides **18b** and **19b** inhibited phosphorylation of SMAD2 (Figure 4D, columns 9

and 10), whereas bicyclic peptides **14b**–**17b** exhibited no activity (Figure 4D columns 5–8and Figure S11B). As **19b** exhibited robust and reproducible inhibition of phosphorylation (Figure S11B), we further tested the ability of **19b** to suppress the NODAL-induced proliferation of ovarian cancer cells. We transfected ovarian cancer cells (Tky-nu) with a plasmid vector containing human NODAL and used a GFP transfected Tky-nu cell line as an isotype control. Tky-nu-NODAL and Tky-nu-GFP cell lines were cultured in the presence and absence of **19b** for 72 hours. Treatment of Tky-nu-GFP cell with 10 μM **19b** had no effect on the proliferation, whereas the viability of Tky-nu-NODAL cells was reduced to 23% when compared to untreated Tky-nu-NODAL cells (Figure 4E). The response to **19b** was dose-dependent with apparent IC50 between 0.1 and 1 μM **19b** (Figure 4E and S13B). The discovery of **19b** served as a promising starting point for developing more potent NODAL antagonists.

Proteolytic stability of bicycles. Intrinsic proteolytic stability of the bicyclic scaffold was critical to the evaluation of the NODAL antagonist in the aforementioned cell-based assays. Specifically, we found that 53% of the bicyclic peptide antagonist **19b** remained intact after 72 hours of incubation at 37 °C in a serum-rich culture medium (Figure S14). We followed up on this observation and tested the stability of a panel of bicyclic scaffolds in various proteolytic degradation conditions (Figure 5). We exposed the bicycles for 5 hours at 37 °C to Pronase™: a mixture of endo- and exo-proteases known to cleave proteins into individual amino acids. The analysis of 21 other **TSL**s bicycles (Figure 5A) highlighted that 25–90% of the bicycles remain intact after 5 hours of exposure to Pronase™ (Figures S15–S22). In these conditions all the tested linear and monocyclic disulfides degraded to <1%. When ten of these bicycles were exposed to fresh mouse serum at 37 °C, on average, 72% of the starting amount was intact after 5 hours (Figures 5A and S22–S23). Monocyclic peptides formed by modifying peptides by (α-α'-dibromo-*m*-xylene) **DBMB**[75-76] have the same topology as one of the rings in **TSL**-modified bicycles. We observed that on average 13% of the **DBMB** macrocycles remained intact after 5-hour treatment by Pronase™, compared to 62% from the **TSL**s-modified set (Figures 5B and S24–S27, the values represent average from the set

of n=14 sequences modified by **DBMB** or **TSL**s). Figure 5C represents an example of bicycle **6b** that remained 83±6.9% intact after 5 h of incubation in Pronase™; the **DBMB** macrocycle **6g** and the disulfide precursor **6a** degraded to <1% under the same conditions. We tested the stability of two sequences modified with the **PFS** cross-linker developed by the Pentelute Lab.[77] In Pronase™, macrocycle **PFS**-STCQGECGGG and bicycle **TSL-3**-STCQGECGGG exhibited similar stability, whereas macrocycle **PFS**-SICRFFCGGG exhibited lower stability than bicycle **TSL-3**-SICRFFCGGG (Figures 5B, S28, and S29). Due to differences in the shape of the cross-linkers resulting in different conformations of peptides, the results were difficult to interpret and we did not expand on this comparison further. In general, it is not trivial to quantify the advantages of any peptide cross-linker in comparison to all other available cross-linkers to-date; however, a comparison of a set of n=14 peptides modified with closely related **DBMB** and **TSL** linkers indeed suggests that bicyclization yields a significant improvement in stability.

Molecular Dynamics Simulation of Bicycle Structures. In testing the stability of a large, diverse set of bicycles, we observed preliminary linker-dependent and sequence dependent trends in degradation. For example, Pronase™ degradation of peptide SWDYRECYLEC modified with **TSL-1** or **TSL6** linker yielded minor but statistically significant differences: 82±13% and 68±14% intact bicycles after 5 hours (Figure 5A). To explore these differences, we employed molecular dynamics (MD) simulation of the conformational ensemble of these bicycles. The penultimate amino acids in **TSL-1**- SWDYRECYLEC and **TSL-6**- SWDYRECYLEC bicycles yielded different Ramachandran plots describing the dihedral angles for -WDYR- sequences in the first ring. On the other hand, the dihedral angle populations for the -CYLEC- sequence in the second ring were similar (Figure S30). The MD simulation suggested that conformations of two rings are decoupled from one another. Differences in degradation for two bicycles, thus, might originate from the enhanced flexibility in one of the rings. Similar decoupling was observed in in **TSL-1**-SHCVWWDC and **TSL-6**-SHCVWWDC bicycles. The penultimate amino acid, His, exhibited different clustering of the dihedral angles. On the other hand, -VWWD- sequence in the second ring

had similar backbone conformations in both bicycles (Figure S30). These studies provide important starting point for understanding ground-state conformational ensemble of these molecules.

CONCLUSION

In conclusion, two-fold symmetric tridentate linchpins that contain aldehyde and two thiol-reactive groups enable a robust one-pot bicyclization of peptides SX_nCX_mC. Such libraries can be used to discover productive antagonists of protein–protein interactions. The bicycles show good stability in digestive conditions. Although the 28 bicyclic peptide sequences tested do not exhaustively sample all possible combinations, the tested peptides included all the potentially problematic amino acids (Lys, Arg, His, Tyr, Trp, Asp/Glu, Ser/Thr). Proteolytic stability of bicyclic architecture sans a free N-terminus is significantly improved when compare to closely-related **DBMB-**cross-linked monocycles. As the strategy is compatible with phage display libraries containing the SX_nCX_mC motif, we anticipate that other peptide libraries that contain this motif will be amenable to such late-stage functionalization. We noted that many genetically encoded libraries do not contain N-terminal Ser and instead have an N-terminal Met or Met analogs encoded by AUC starting codon. However, it is possible to introduce an N-terminal Ser into these systems by expressing a library with N-terminal TEV-cleavable sequence: H-MENLYFQ\S (where \ denoted as the cleavage site). A conceptually similar approach has been recently demonstrated by Jianmin Gao and co-workers who expressed ENLYFQ\C in phage libraries and used TEV cleavage to expose the N-terminal Cys.[78] Finally, the lower symmetry of the **TSL**-style linkers allows their diversification with any chemotype of C_2-symmetry.[71] It offers a significant expansion of the bicyclization repertoire beyond traditional architectures produced from three-fold symmetric cross-linkers.

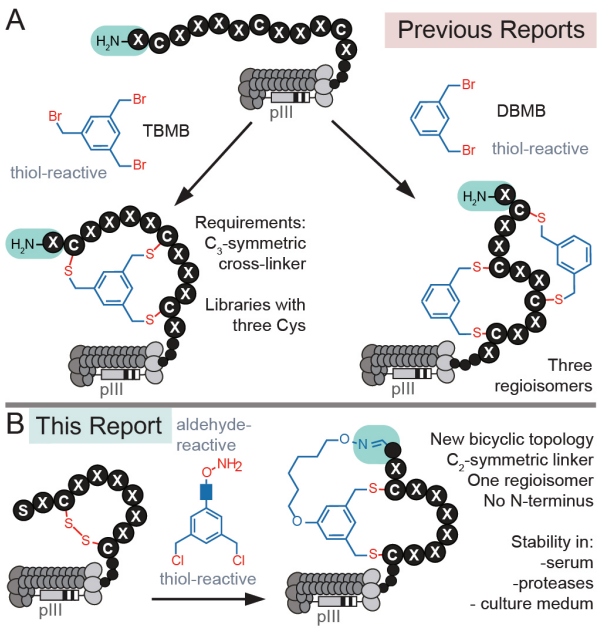

Figure 1: (A) Previous reports of created bicyclic peptides on the M13 phage display library. (B) The approach of this report for generating bicyclic peptides on the M13 phage display library.

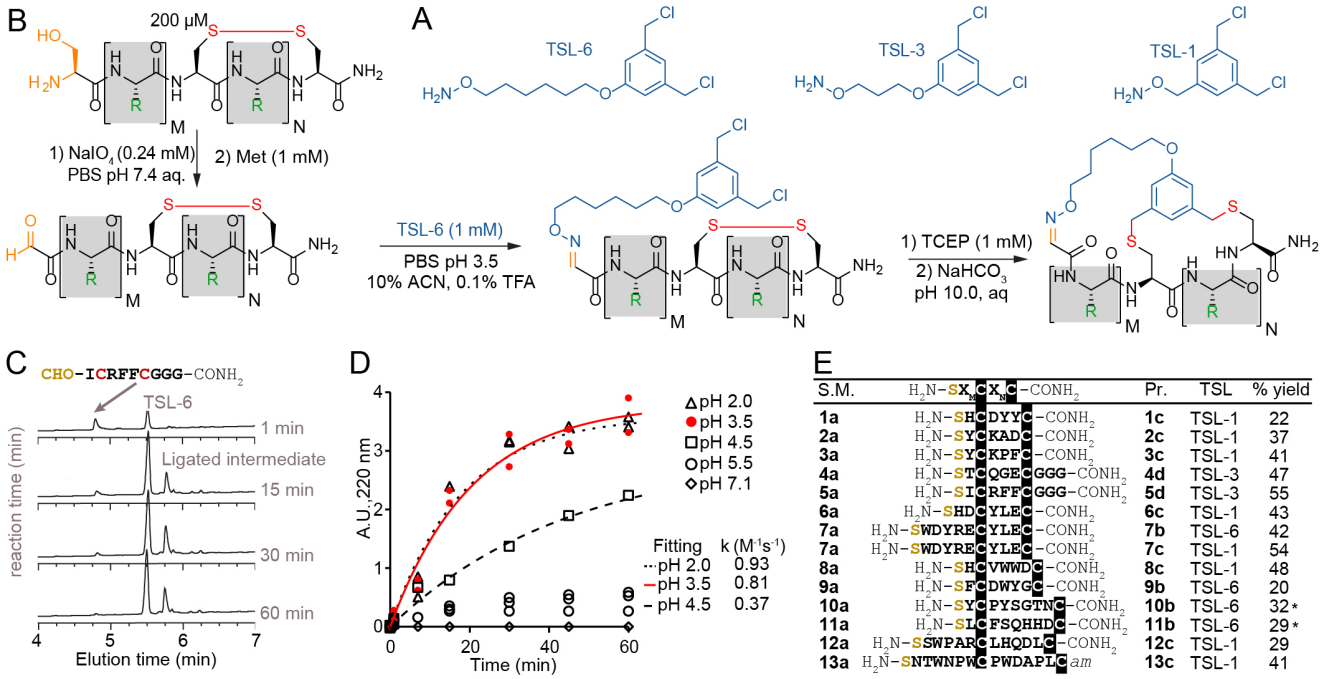

Figure 2: Macrocyclization reaction of bicycles with model peptides. (A) Chemical structure of **TSL**s. (B) Ligation of disulfide peptides with **TSL-6** at pH 3.5 and further macrocyclization into bicyclic peptides at pH 10. (C) Liquid chromatography traces at 220 nM for the reaction between oxidated **5a** and **TSL-6**. The reaction reaches 95% completion in 1 hour. (D) Kinetic traces of the reaction between oxidated **5a** and **TSL-6** at different pH. Reaction rates at pH 2.0, pH 3.5, and pH 4.5 were fit to pseudo first order kinetic equation to determine k values. (E) Isolated yields of bicyclic peptides with various sequences and different **TSL**s. (*see supporting information page S20-S21 for details of the modification protocol)

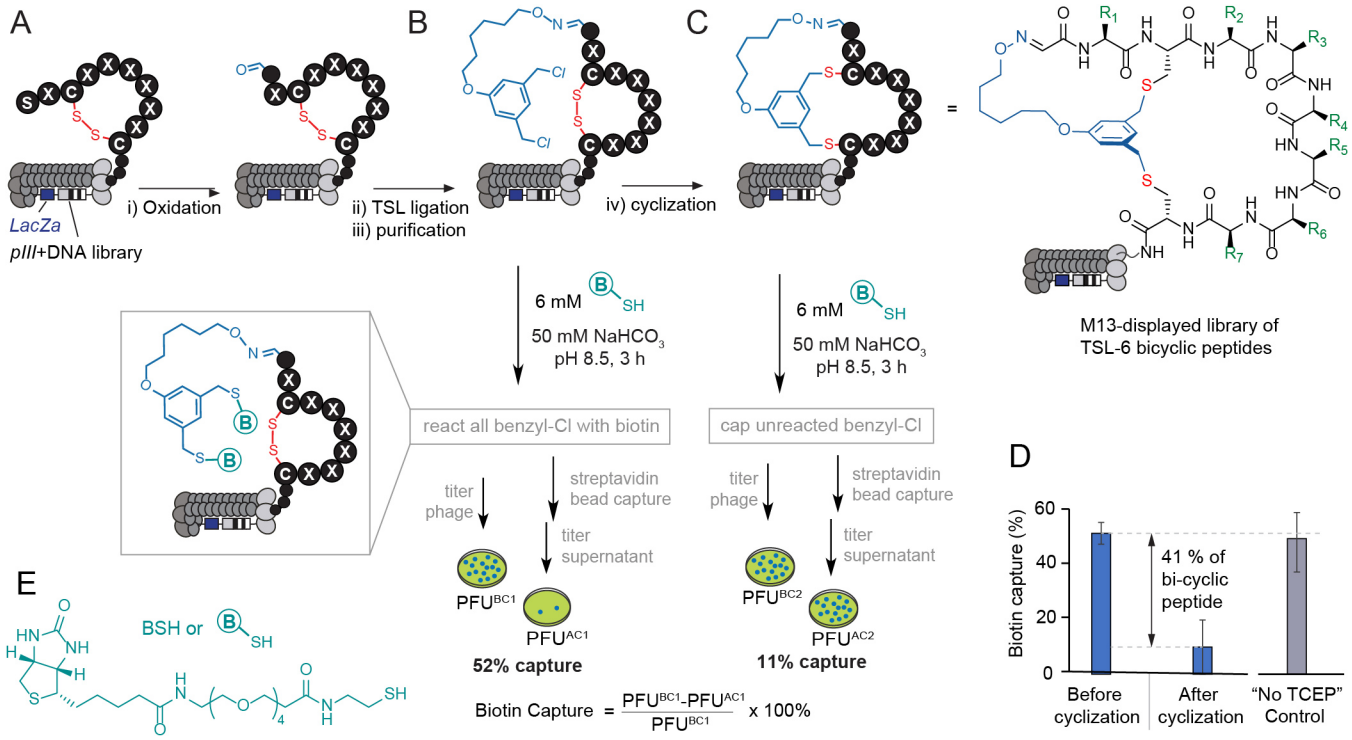

Figure 3: Modification of the library of 10^8 peptides displayed on phage by the **TSL-6**. (A–B) M13 phage displayed disulfide library was oxidated and ligated with **TSL-6**. (C) The **TSL-6** ligated peptides were further converted into bicyclic peptides. (D) Quantification of phage with thiol-reactive groups before and after cyclization. Control incubation of **TSL-6**-ligated phage in pH 10 buffer for 3 h did not lead to a significant decrease of thiol-reactive group content. (E) Chemical structure of the biotin-thiol (BSH) probe.

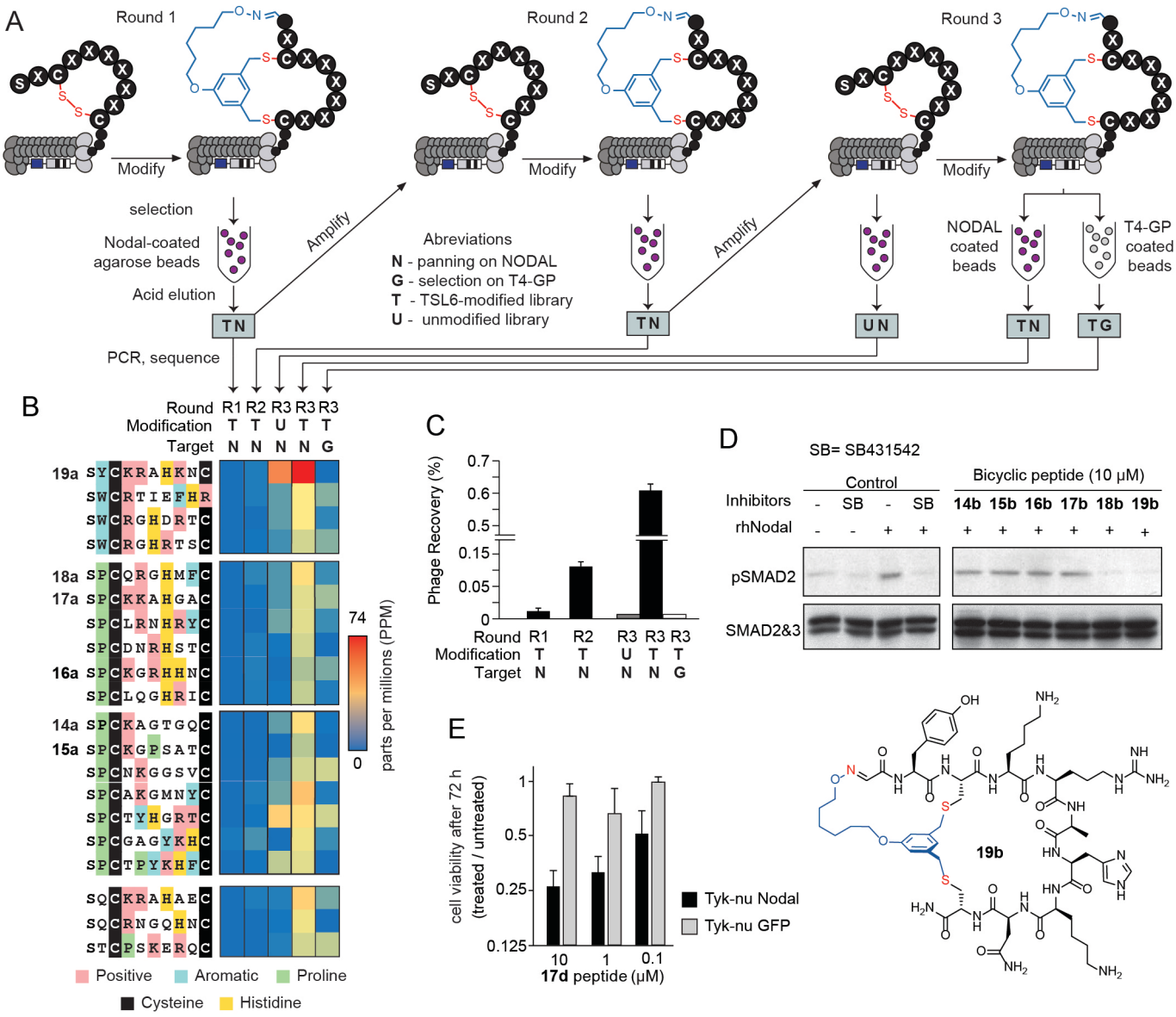

Figure 4: Bio-panning against the NODAL protein. (A) A scheme of three-round panning against NODAL and negative controls. (B) The top 20 sequences from the deep sequencing results were clustered into 4 groups and 6 of them were chemically synthesized. (C) Percentage of the phage recovery after each round of bio-panning. (D) Western blot measuring the response of p-SMAD2 in P19 cells to treatment with rhNODAL and inhibitors. Total SMAD was used as control. (E) Cell viability assay of Tky-nu cell line transfected with rhNODAL or GFP and treated with **19b** at various peptide concentrations for 72 hr.

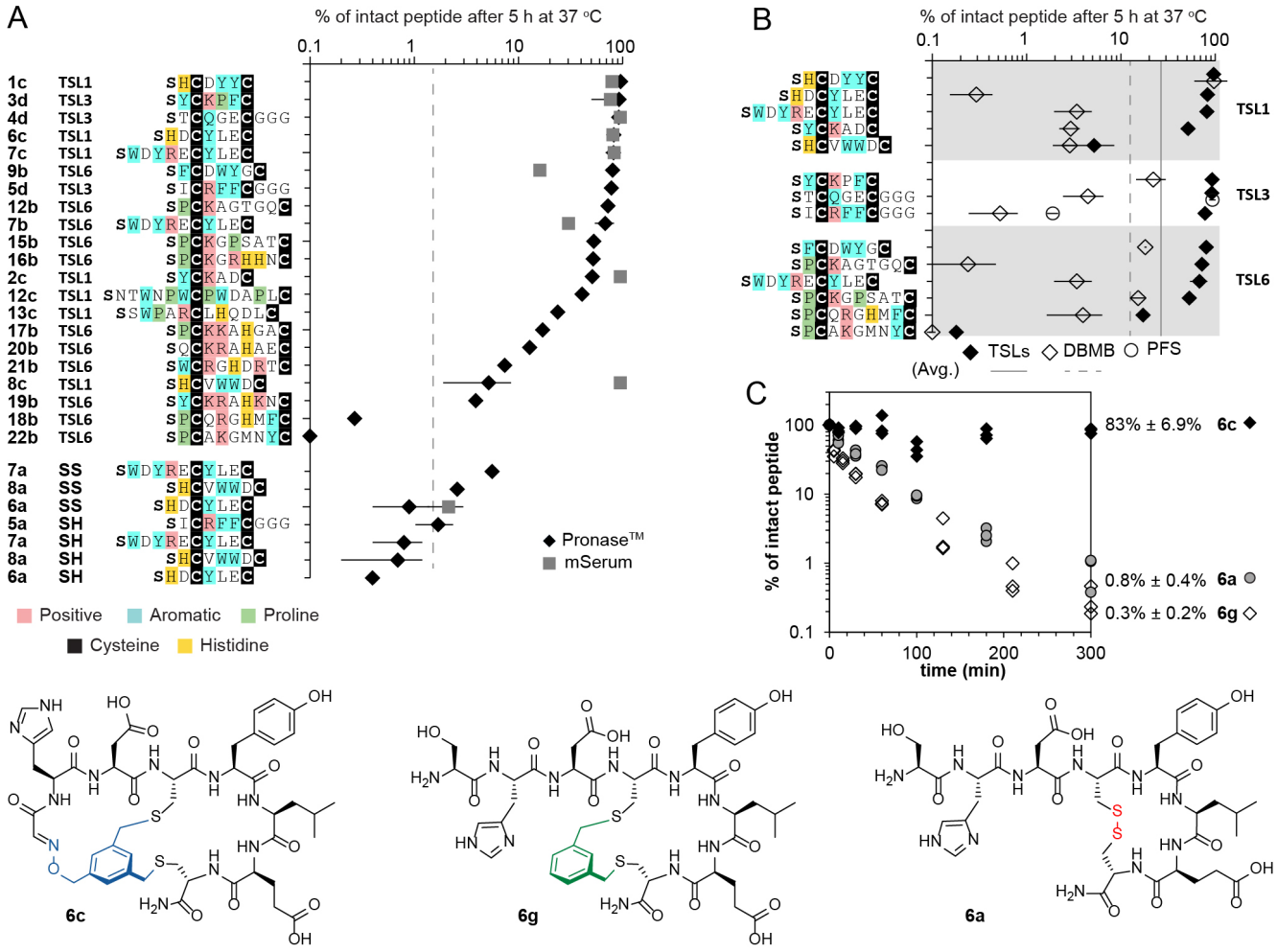

Figure 5: Proteolytic stability of bicycles and controls. (A) Stability of **TSL**s bicycles, disulfide constrained peptides, and linear peptides in the presence of Pronase™ and mouse serum for 5 h at 37 °C. (B) Stability of peptides modified with **TSLs**, **DBMB** and **PFS** in the presence of Pronase™ for 5 h at 37 °C. (C) Stability of **6a** (disulfide-bonded), **6c** (bicycled with **TSL-1**), and **6g** (macro-cyclized with **DBMB**) in the presence of Pronase™.

ASSOCIATED CONTENT

Supporting Information. Details of synthesis and characterization, materials and methods, supplementary schemes, tables, and figures (PDF).

Funding Sources

This work was supported by funding from the Ferring Research Institute (to R.D.), NSERC (RGPIN-2016-402511 to R.D.), NSERC Accelerator Supplement (to R.D.), Canadian Institutes of Health Research (CIHR FRN: 168961, to R.D.), and the National Institute of General Medical Sciences of the National Institutes of Health (R01GM124160 to Y.-S.L.). Infrastructure support was provided by CFI New Leader Opportunity (to R.D.).

Notes

Conflict of interest statement: Patent application describing this invention was filed by TEC Edmonton in July 2018. R.D. is a shareholder of 48Hour Discovery Inc., the company licensing the technology.

Acknowledgments

We thank Prof. Rylan Lundgren and Samantha Kwok for their critical review of the paper, Dr. R. Whittal and B. Reiz for assistance with mass spectroscopic studies, and Susmita Sarkar for providing the mouse serum.

REFERENCES

1. Vlieghe, P.; Lisowski, V.; Martinez, J.; Khrestchatisky, M., Synthetic therapeutic peptides: science and market. *Drug Discov. Today* **2010,** *15* (1-2), 40-56.

2. Lofblom, J.; Feldwisch, J.; Tolmachev, V.; Carlsson, J.; Stahl, S.; Frejd, F. Y., Affibody molecules: engineered proteins for therapeutic, diagnostic and biotechnological applications. *FEBS Lett.* **2010,** *584* (12), 2670-80.

3. Lian, W.; Upadhyaya, P.; Rhodes, C. A.; Liu, Y.; Pei, D., Screening bicyclic peptide libraries for protein-protein interaction inhibitors: discovery of a tumor necrosis factor-alpha antagonist. *J. Am. Chem. Soc.* **2013,** *135* (32), 11990-5.

4. Villar, E. A.; Beglov, D.; Chennamadhavuni, S.; Porco, J. A., Jr.; Kozakov, D.; Vajda, S.; Whitty, A., How proteins bind macrocycles. *Nat. Chem. Biol.* **2014,** *10* (9), 723-31.

5. Heinis, C.; Rutherford, T.; Freund, S.; Winter, G., Phage-encoded combinatorial chemical libraries based on bicyclic peptides. *Nat. Chem. Biol.* **2009,** *5* (7), 502-7.

6. Roxin, A.; Zheng, G., Flexible or fixed: a comparative review of linear and cyclic cancer-targeting peptides. *Future Med. Chem.* **2012,** *4* (12), 1601-18.

7. Craik, D. J.; Fairlie, D. P.; Liras, S.; Price, D., The future of peptide-based drugs. *Chem. Biol. Drug Des.* **2013,** *81* (1), 136-47.

8. Robinson, J. A.; Demarco, S.; Gombert, F.; Moehle, K.; Obrecht, D., The design, structures and therapeutic potential of protein epitope mimetics. *Drug Discov. Today* **2008,** *13* (21-22), 944-51.

9. Gao, Y.; Kodadek, T., Direct comparison of linear and macrocyclic compound libraries as a source of protein ligands. *ACS Comb. Sci.* **2015,** *17* (3), 190-5.

10. Hacker, D. E.; Abrigo, N. A.; Hoinka, J.; Richardson, S. L.; Przytycka, T. M.; Hartman, M. C. T., Direct, Competitive Comparison of Linear, Monocyclic, and Bicyclic Libraries Using mRNA Display. *ACS Comb. Sci.* **2020,** *22* (6), 306-310.

11. Matinkhoo, K.; Pryyma, A.; Todorovic, M.; Patrick, B. O.; Perrin, D. M., Synthesis of the Death-Cap Mushroom Toxin alpha-Amanitin. *J. Am. Chem. Soc.* **2018,** *140* (21), 6513-6517.

12. Hosseinzadeh, P.; Bhardwaj, G.; Mulligan, V. K.; Shortridge, M. D.; Craven, T. W.; Pardo-Avila, F.; Rettie, S. A.; Kim, D. E.; Silva, D. A.; Ibrahim, Y. M.; Webb, I. K.; Cort, J. R.; Adkins, J. N.; Varani, G.; Baker, D., Comprehensive computational design of ordered peptide macrocycles. *Science* **2017,** *358* (6369), 1461-1466.

13. Richelle, G. J. J.; Schmidt, M.; Ippel, H.; Hackeng, T. M.; van Maarseveen, J. H.; Nuijens, T.; Timmerman, P., A One-Pot "Triple-C" Multicyclization Methodology for the Synthesis of Highly Constrained Isomerically Pure Tetracyclic Peptides. *ChemBioChem* **2018,** *19* (18), 1934-1938.

14. Wolfe, J. M.; Fadzen, C. M.; Holden, R. L.; Yao, M.; Hanson, G. J.; Pentelute, B. L., Perfluoroaryl Bicyclic Cell-Penetrating Peptides for Delivery of Antisense Oligonucleotides. *Angew. Chem. Int. Ed. Engl.* **2018,** *57* (17), 4756-4759.

15. Liu, W.; Zheng, Y.; Kong, X.; Heinis, C.; Zhao, Y.; Wu, C., Precisely Regulated and Efficient Locking of Linear Peptides into Stable Multicyclic Topologies through a One-Pot Reaction. *Angew. Chem. Int. Ed. Engl.* **2017,** *56* (16), 4458-4463.

16. Trinh, T. B.; Upadhyaya, P.; Qian, Z.; Pei, D., Discovery of a Direct Ras Inhibitor by Screening a Combinatorial Library of Cell-Permeable Bicyclic Peptides. *ACS Comb. Sci.* **2016,** *18* (1), 75-85.

17. Morimoto, J.; Kodadek, T., Synthesis of a large library of macrocyclic peptides containing multiple and diverse N-alkylated residues. *Mol. Biosyst.* **2015,** *11* (10), 2770-9.

18. Franzini, R. M.; Neri, D.; Scheuermann, J., DNA-encoded chemical libraries: advancing beyond conventional small-molecule libraries. *Acc. Chem. Res.* **2014,** *47* (4), 1247-55.

19. Li, Y.; De Luca, R.; Cazzamalli, S.; Pretto, F.; Bajic, D.; Scheuermann, J.; Neri, D., Versatile protein recognition by the encoded display of multiple chemical elements on a constant macrocyclic scaffold. *Nat. Chem.* **2018,** *10* (4), 441-448.

20. Denton, K. E.; Wang, S.; Gignac, M. C.; Milosevich, N.; Hof, F.; Dykhuizen, E. C.; Krusemark, C. J., Robustness of In Vitro Selection Assays of DNA-Encoded Peptidomimetic Ligands to CBX7 and CBX8. *SLAS Discov.* **2018,** *23* (5), 417-428.

21. Millward, S. W.; Takahashi, T. T.; Roberts, R. W., A general route for post-translational cyclization of mRNA display libraries. *J. Am. Chem. Soc.* **2005,** *127* (41), 14142-3.

22. Bellotto, S.; Chen, S.; Rentero Rebollo, I.; Wegner, H. A.; Heinis, C., Phage selection of photoswitchable peptide ligands. *J. Am. Chem. Soc.* **2014,** *136* (16), 5880-3.

23. Jafari, M. R.; Deng, L.; Kitov, P. I.; Ng, S.; Matochko, W. L.; Tjhung, K. F.; Zeberoff, A.; Elias, A.; Klassen, J. S.; Derda, R., Discovery of light-responsive ligands through screening of a light-responsive genetically encoded library. *ACS Chem. Biol.* **2014,** *9* (2), 443-50.

24. Jafari, M. R.; Lakusta, J.; Lundgren, R. J.; Derda, R., Allene Functionalized Azobenzene Linker Enables Rapid and Light-Responsive Peptide Macrocyclization. *Bioconjugate Chem.* **2016,** *27* (3), 509-14.

25. Yang, L.; Zhenkun, N.; Sarah A., S.; Matthew D., S.; Jeremy A., S.; Tanja, H., Discovery of cellular substrates of human RNA decapping enzyme Dcp2 using a stapled bicyclic peptide inhibitor. *ChemRxiv*, October 20, 2020, Ver 4, DOI: 10.26434/chemrxiv.12233102.v4, (accessed 2021-02-08).

26. Hetrick, K. J.; Walker, M. C.; van der Donk, W. A., Development and Application of Yeast and Phage Display of Diverse Lanthipeptides. *ACS Cent Sci* **2018,** *4* (4), 458-467.

27. Derda, R.; Jafari, M. R., Synthetic Cross-linking of Peptides: Molecular Linchpins for Peptide Cyclization. *Protein Pept. Lett.* **2018,** *25* (12), 1051-1075.

28. Zorzi, A.; Deyle, K.; Heinis, C., Cyclic peptide therapeutics: past, present and future. *Curr. Opin. Chem. Biol.* **2017,** *38*, 24-29.

29. Kong, X. D.; Moriya, J.; Carle, V.; Pojer, F.; Abriata, L. A.; Deyle, K.; Heinis, C., De novo development of proteolytically resistant therapeutic peptides for oral administration. *Nat. Biomed. Eng.* **2020,** *4* (5), 560-571.

30. Hacker, D. E.; Hoinka, J.; Iqbal, E. S.; Przytycka, T. M.; Hartman, M. C., Highly Constrained Bicyclic Scaffolds for the Discovery of Protease-Stable Peptides via mRNA Display. *ACS Chem. Biol.* **2017,** *12* (3), 795-804.

31. Hartman, M. C.; Josephson, K.; Lin, C. W.; Szostak, J. W., An expanded set of amino acid analogs for the ribosomal translation of unnatural peptides. *PLoS One* **2007,** *2* (10), e972.

32. Tian, F.; Tsao, M. L.; Schultz, P. G., A phage display system with unnatural amino acids. *J. Am. Chem. Soc.* **2004,** *126* (49), 15962-3.

33. Oller-Salvia, B.; Chin, J. W., Efficient Phage Display with Multiple Distinct Non-Canonical Amino Acids Using Orthogonal Ribosome-Mediated Genetic Code Expansion. *Angew. Chem. Int. Ed. Engl.* **2019,** *58* (32), 10844-10848.

34. Wang, X. S.; Chen, P. C.; Hampton, J. T.; Tharp, J. M.; Reed, C. A.; Das, S. K.; Wang, D. S.; Hayatshahi, H. S.; Shen, Y.; Liu, J.; Liu, W. R., A Genetically Encoded, Phage-Displayed Cyclic-Peptide Library. *Angew. Chem. Int. Ed. Engl.* **2019,** *58* (44), 15904-15909.

35. Owens, A. E.; Iannuzzelli, J. A.; Gu, Y.; Fasan, R., MOrPH-PhD: An Integrated Phage Display Platform for the Discovery of Functional Genetically Encoded Peptide Macrocycles. *ACS Cent Sci* **2020,** *6* (3), 368-381.

36. Yao, A.; Reed, S. A.; Koh, M.; Yu, C.; Luo, X.; Mehta, A. P.; Schultz, P. G., Progress toward a reduced phage genetic code. *Bioorg. Med. Chem.* **2018,** *26* (19), 5247-5252.

37. Nicolet, B. H.; Shinn, L. A., The Action of Periodic Acid on α-Amino Alcohols. *J. Am. Chem. Soc.* **1939,** *61* (6), 1615-1615.

38. Geoghegan, K. F.; Stroh, J. G., Site-directed conjugation of nonpeptide groups to peptides and proteins via periodate oxidation of a 2-amino alcohol. Application to modification at N-terminal serine. *Bioconjugate Chem.* **1992,** *3* (2), 138-46.

39. Clamp, J. R.; Hough, L., The Periodate Oxidation of Amino Acids with Reference to Studies on Glycoproteins. *Biochem. J.* **1965,** *94* (1), 17-24.

40. Bai, C.; Reid, E. E.; Wilhelm, A.; Shizuka, M.; Maloney, E. K.; Laleau, R.; Harvey, L.; Archer, K. E.; Vitharana, D.; Adams, S.; Kovtun, Y.; Miller, M. L.; Chari, R.; Keating, T. A.; Yoder, N. C., Site-Specific Conjugation of the Indolinobenzodiazepine DGN549 to Antibodies Affords Antibody-Drug Conjugates with an Improved Therapeutic Index as Compared with Lysine Conjugation. *Bioconjugate Chem.* **2020,** *31* (1), 93-103.

41. Gaertner, H. F.; Offord, R. E., Site-specific attachment of functionalized poly(ethylene glycol) to the amino terminus of proteins. *Bioconjugate Chem.* **1996,** *7* (1), 38-44.

42. Nie, Y.; Zhang, X.; Wang, X.; Chen, J., Preparation and stability of N-terminal mono-PEGylated recombinant human endostatin. *Bioconjugate Chem.* **2006,** *17* (4), 995-9.

43. Ng, S.; Lin, E.; Kitov, P. I.; Tjhung, K. F.; Gerlits, O. O.; Deng, L.; Kasper, B.; Sood, A.; Paschal, B. M.; Zhang, P.; Ling, C. C.; Klassen, J. S.; Noren, C. J.; Mahal, L. K.; Woods, R. J.; Coates, L.; Derda, R., Genetically encoded fragment-based discovery of glycopeptide ligands for carbohydrate-binding proteins. *J. Am. Chem. Soc.* **2015,** *137* (16), 5248-51.

44. Chou, Y.; Kitova, E. N.; Joe, M.; Brunton, R.; Lowary, T. L.; Klassen, J. S.; Derda, R., Genetically-encoded fragment-based discovery (GE-FBD) of glycopeptide ligands with differential selectivity for antibodies related to mycobacterial infections. *Org. Biomol. Chem.* **2018,** *16* (2), 223-227.

45. Kitov, P. I.; Vinals, D. F.; Ng, S.; Tjhung, K. F.; Derda, R., Rapid, hydrolytically stable modification of aldehyde-terminated proteins and phage libraries. *J. Am. Chem. Soc.* **2014,** *136* (23), 8149-52.

46. Triana, V.; Derda, R., Tandem Wittig/Diels-Alder diversification of genetically encoded peptide libraries. *Org. Biomol. Chem.* **2017,** *15* (37), 7869-7877.

47. Vinals, D. F.; Kitov, P. I.; Tu, Z.; Zou, C.; Cairo, C. W.; Lin, H. C.-H.; Derda, R., Selection of galectin-3 ligands derived from genetically encoded glycopeptide libraries. *Pept. Sci.* **2019,** *111* (1), e24097.

48. Ng, S.; Bennett, N. J.; Schulze, J.; Gao, N.; Rademacher, C.; Derda, R., Genetically-encoded fragment-based discovery of glycopeptide ligands for DC-SIGN. *Bioorg. Med. Chem.* **2018,** *26* (19), 5368-5377.

49. Jafari, M. R.; Yu, H.; Wickware, J. M.; Lin, Y. S.; Derda, R., Light-responsive bicyclic peptides. *Org. Biomol. Chem.* **2018,** *16* (41), 7588-7594.

50. Tjhung, K. F.; Kitov, P. I.; Ng, S.; Kitova, E. N.; Deng, L.; Klassen, J. S.; Derda, R., Silent Encoding of Chemical Post-Translational Modifications in Phage-Displayed Libraries. *J. Am. Chem. Soc.* **2016,** *138* (1), 32-5.

51. Ng, S.; Jafari, M. R.; Matochko, W. L.; Derda, R., Quantitative synthesis of genetically encoded glycopeptide libraries displayed on M13 phage. *ACS Chem. Biol.* **2012,** *7* (9), 1482-7.

52. Lonardo, E.; Hermann, P. C.; Mueller, M. T.; Huber, S.; Balic, A.; Miranda-Lorenzo, I.; Zagorac, S.; Alcala, S.; Rodriguez-Arabaolaza, I.; Ramirez, J. C.; Torres-Ruiz, R.; Garcia, E.; Hidalgo, M.; Cebrian, D. A.; Heuchel, R.; Lohr, M.; Berger, F.; Bartenstein, P.; Aicher, A.; Heeschen, C., Nodal/Activin signaling drives self-renewal and tumorigenicity of pancreatic cancer stem cells and provides a target for combined drug therapy. *Cell stem cell* **2011,** *9* (5), 433-46.

53. Kirsammer, G.; Strizzi, L.; Margaryan, N. V.; Gilgur, A.; Hyser, M.; Atkinson, J.; Kirschmann, D. A.; Seftor, E. A.; Hendrix, M. J., Nodal signaling promotes a tumorigenic phenotype in human breast cancer. *Semin. Cancer Biol.* **2014,** *29*, 40-50.

54. Gong, Y.; Guo, Y.; Hai, Y.; Yang, H.; Liu, Y.; Yang, S.; Zhang, Z.; Ma, M.; Liu, L.; Li, Z.; He, Z., Nodal promotes the self-renewal of human colon cancer stem cells via an autocrine manner through Smad2/3 signaling pathway. *BioMed Res. Int.* **2014,** *2014*, 364134.

55. Strizzi, L.; Hardy, K. M.; Margaryan, N. V.; Hillman, D. W.; Seftor, E. A.; Chen, B.; Geiger, X. J.; Thompson, E. A.; Lingle, W. L.; Andorfer, C. A.; Perez, E. A.; Hendrix, M. J., Potential for the embryonic morphogen Nodal as a prognostic and predictive biomarker in breast cancer. *Breast Cancer Res.* **2012,** *14* (3), R75.

56. Topczewska, J. M.; Postovit, L. M.; Margaryan, N. V.; Sam, A.; Hess, A. R.; Wheaton, W. W.; Nickoloff, B. J.; Topczewski, J.; Hendrix, M. J., Embryonic and tumorigenic pathways converge via Nodal signaling: role in melanoma aggressiveness. *Nat. Med.* **2006,** *12* (8), 925-32.

57. Lee, C. C.; Jan, H. J.; Lai, J. H.; Ma, H. I.; Hueng, D. Y.; Lee, Y. C.; Cheng, Y. Y.; Liu, L. W.; Wei, H. W.; Lee, H. M., Nodal promotes growth and invasion in human gliomas. *Oncogene* **2010,** *29* (21), 3110-23.

58. Lawrence, M. G.; Margaryan, N. V.; Loessner, D.; Collins, A.; Kerr, K. M.; Turner, M.; Seftor, E. A.; Stephens, C. R.; Lai, J.; BioResource, A. P. C.; Postovit, L.-M.; Clements, J. A.; Hendrix, M. J. C., Reactivation of embryonic nodal signaling is associated with tumor progression and promotes the growth of prostate cancer cells. *Prostate* **2011,** *71* (11), 1198-1209.

59. Cavallari, C.; Fonsato, V.; Herrera, M. B.; Bruno, S.; Tetta, C.; Camussi, G., Role of Lefty in the anti tumor activity of human adult liver stem cells. *Oncogene* **2013,** *32* (7), 819-26.

60. Chen, J.; Liu, W. B.; Jia, W. D.; Xu, G. L.; Ma, J. L.; Ren, Y.; Chen, H.; Sun, S. N.; Huang, M.; Li, J. S., Embryonic morphogen nodal is associated with progression and poor prognosis of hepatocellular carcinoma. *PLoS One* **2014,** *9* (1), e85840.

61. Law, J.; Zhang, G.; Dragan, M.; Postovit, L. M.; Bhattacharya, M., Nodal signals via beta-arrestins and RalGTPases to regulate trophoblast invasion. *Cell. Signal.* **2014,** *26* (9), 1935-42.

62. Kong, B.; Wang, W.; Esposito, I.; Friess, H.; Michalski, C. W.; Kleeff, J., Increased expression of Nodal correlates with reduced patient survival in pancreatic cancer. *Pancreatology* **2015,** *15* (2), 156-61.

63. Quail, D. F.; Siegers, G. M.; Jewer, M.; Postovit, L. M., Nodal signalling in embryogenesis and tumourigenesis. *Int. J. Biochem. Cell Biol.* **2013,** *45* (4), 885-98.

64. Hendrix, M. J.; Seftor, E. A.; Seftor, R. E.; Kasemeier-Kulesa, J.; Kulesa, P. M.; Postovit, L. M., Reprogramming metastatic tumour cells with embryonic microenvironments. *Nat. Rev. Cancer* **2007,** *7* (4), 246-55.

65. Grimes, D. T.; Burdine, R. D., Left-Right Patterning: Breaking Symmetry to Asymmetric Morphogenesis. *Trends Genet.* **2017,** *33* (9), 616-628.

66. Hooijkaas, A. I.; Gadiot, J.; van Boven, H.; Blank, C., Expression of the embryological morphogen Nodal in stage III/IV melanoma. *Melanoma Res.* **2011,** *21* (6), 491-501.

67. Quail, D. F.; Zhang, G.; Walsh, L. A.; Siegers, G. M.; Dieters-Castator, D. Z.; Findlay, S. D.; Broughton, H.; Putman, D. M.; Hess, D. A.; Postovit, L. M., Embryonic morphogen nodal promotes breast cancer growth and progression. *PLoS One* **2012,** *7* (11), e48237.

68. Lonardo, E.; Hermann, P. C.; Mueller, M. T.; Huber, S.; Balic, A.; Miranda-Lorenzo, I.; Zagorac, S.; Alcala, S.; Rodriguez-Arabaolaza, I.; Ramirez, J. C.; Torres-Ruíz, R.; Garcia, E.; Hidalgo, M.; Cebrián, D.; Heuchel, R.; Löhr, M.; Berger, F.; Bartenstein, P.; Aicher, A.; Heeschen, C., Nodal/Activin signaling drives self-renewal and tumorigenicity of pancreatic cancer stem cells and provides a target for combined drug therapy. *Cell stem cell* **2011,** *9* (5), 433-46.

69. Strizzi, L.; Sandomenico, A.; Margaryan, N. V.; Foca, A.; Sanguigno, L.; Bodenstine, T. M.; Chandler, G. S.; Reed, D. W.; Gilgur, A.; Seftor, E. A.; Seftor, R. E.; Khalkhali-Ellis, Z.; Leonardi, A.; Ruvo, M.; Hendrix, M. J., Effects of a novel Nodal-targeting monoclonal antibody in melanoma. *Oncotarget* **2015,** *6* (33), 34071-86.

70. Dirksen, A.; Dawson, P. E., Rapid Oxime and Hydrazone Ligations with Aromatic Aldehydes for Biomolecular Labeling. *Bioconjugate Chem.* **2008,** *19* (12), 2543-2548.

71. Jafari, M. R.; Yu, H.; Wickware, J. M.; Lin, Y.-S.; Derda, R., Light-responsive bicyclic peptides. *Org. Biomol. Chem.* **2018**.

72. Teufel, D. P.; Bennett, G.; Harrison, H.; van Rietschoten, K.; Pavan, S.; Stace, C.; Le Floch, F.; Van Bergen, T.; Vermassen, E.; Barbeaux, P.; Hu, T. T.; Feyen, J. H. M.; Vanhove, M., Stable and Long-Lasting, Novel Bicyclic Peptide Plasma Kallikrein Inhibitors for the Treatment of Diabetic Macular Edema. *J. Med. Chem.* **2018,** *61* (7), 2823-2836.

73. Quail, D. F.; Taylor, M. J.; Walsh, L. A.; Dieters-Castator, D.; Das, P.; Jewer, M.; Zhang, G.; Postovit, L. M., Low oxygen levels induce the expression of the embryonic morphogen Nodal. *Mol. Biol. Cell* **2011,** *22* (24), 4809-21.

74. Quail, D. F.; Zhang, G.; Findlay, S. D.; Hess, D. A.; Postovit, L. M., Nodal promotes invasive phenotypes via a mitogen-activated protein kinase-dependent pathway. *Oncogene* **2014,** *33* (4), 461-73.

75. Diderich, P.; Bertoldo, D.; Dessen, P.; Khan, M. M.; Pizzitola, I.; Held, W.; Huelsken, J.; Heinis, C., Phage Selection of Chemically Stabilized alpha-Helical Peptide Ligands. *ACS Chem. Biol.* **2016,** *11* (5), 1422-7.

76. Timmerman, P.; Beld, J.; Puijk, W. C.; Meloen, R. H., Rapid and quantitative cyclization of multiple peptide loops onto synthetic scaffolds for structural mimicry of protein surfaces. *ChemBioChem* **2005,** *6* (5), 821-4.

77. Zou, Y.; Spokoyny, A. M.; Zhang, C.; Simon, M. D.; Yu, H.; Lin, Y. S.; Pentelute, B. L., Convergent diversity-oriented side-chain macrocyclization scan for unprotected polypeptides. *Org. Biomol. Chem.* **2014,** *12* (4), 566-73.

78. Li, K.; Wang, W.; Gao, J., Fast and Stable N-Terminal Cysteine Modification through Thiazolidino Boronate Mediated Acyl Transfer. *Angew. Chem. Int. Ed. Engl.* **2020,** *59* (34), 14246-14250.